

5/20/89  
82183

# Phase Distribution Phenomena for Simulated Microgravity Conditions: Experimental Work

Maneesh Singhal, Fabian J. Bonetto, R.T. Lahey Jr.  
Center For Multiphase Flow, Rensselaer Polytechnic Institute  
Troy, NY 12180

5/15/89  
88

## 1.0 INTRODUCTION

This report summarizes the work accomplished at Rensselaer to study phase distribution phenomenon under simulated microgravity conditions. Our group at Rensselaer has been able to develop sophisticated analytical models to predict phase distribution in two-phase flows under variety of conditions. These models are based on physics and data obtained from carefully controlled experiments that are being conducted here. These experiments also serve to verify the models developed.

## 2.0 ANALYSIS

### 2.1 Conservation Equations

The generic conservation equation for each phase is given by:

$$\frac{\partial}{\partial t} \rho \Psi + \nabla \cdot \rho \Psi \mathbf{v} = \nabla \cdot \mathbf{J} + \rho f \quad (1)$$

The corresponding jump condition between components  $k$  and  $l$  is:

$$[(\rho \Psi (\mathbf{v} - \mathbf{v}_i) + \mathbf{J}) \cdot \mathbf{n}]_{kl} = M_i \quad (2)$$

where:

- $\Psi$  ... conserved quantity
  - $\mathbf{J}$  ... conserved quantity's flux
  - $f$  ... conserved quantity's source density
  - $M_i$  ... conserved quantity's interfacial source
- Typical state variables are given in Table I.

TABLE I State variables in generic conservation equations and jump conditions

Balance Principle	$\Psi$	$\mathbf{J}$	$f$	$M_i$
Mass	1	0	0	0
Momentum	$\mathbf{v}$	$\mathbf{T}$	$\mathbf{g}$	$m_i^s$
Energy	$u + 0.5 \mathbf{v}^2$	$\mathbf{T} \cdot \mathbf{v} - \mathbf{q}$	$\mathbf{g} \cdot \mathbf{v} + r$	$e_i^s$
Enthalpy	$h$	$-\mathbf{q}$	$r + \frac{1}{\rho} \left( \frac{dp}{dt} + \tau : \nabla \mathbf{v} \right)$	$h_i^s$

To obtain the conservation equations which govern the

motion of turbulent dispersed solid/fluid flows, the generic equation is first multiplied by the phase indicator function,  $X_k$ , defined as:

$$X_k = \begin{cases} 1, & \text{if } x \in k \\ 0, & \text{otherwise} \end{cases} \quad (3)$$

and then averaged over all the possible realizations (ensembles). Drew et. al. [1995] define ensemble averaging of a function  $F$  at position  $x$  and time  $t$ , for some particular realization  $\mu$ , as:

$$F(x, t) = \int_{\mathcal{E}} F(x, t; \mu) dm(\mu) \quad (4)$$

where  $\mathcal{E}$ , ensemble, is the set of all the possible realizations. Also, if we consider a point on the interface while moving with it, we see that the phase indicator function,  $X_k$ , is a constant jump discontinuity. Therefore, its material derivative must be zero. That is,

$$\frac{D_t X_k}{Dt} = \frac{\partial X_k}{\partial t} + \mathbf{v}_i \cdot \nabla X_k = 0. \quad (5)$$

By using the above equation and procedure, ensemble-averaged conservation equations for adiabatic two-phase flow are obtained. These have been described in detail elsewhere [Alajbegovic 1994].

### 2.2 Closure

#### 2.2.1 The Interfacial momentum source

The interfacial momentum source can be partitioned into drag and non-drag components [Lahey & Drew, 1990], as:

$$\mathbf{M}_k = -\overline{\mathbf{T} \cdot \nabla X_k} = \mathbf{M}_k^{(D)} + \mathbf{M}_k^{(ND)} \quad (6)$$

For drag we may assume:

$$\mathbf{M}_c^{(D)} = -\mathbf{M}_d^{(D)} = \frac{1}{8} \rho_c C_D |\mathbf{v}_r| \mathbf{v}_r A_i''' \quad (7)$$

The non-drag component may be obtained assuming inviscid flow around spherical particles [Arnold, 1988; Park, 1992]. The average quantities were obtained using cell-averaging techniques [Nigmatulin, 1979], which are an approximation to ensemble averaging. The resulting expression includes virtual mass effects and a lateral force induced by the

non-uniform flow field around a spherical particle. The latter force is called lift force and is given by [Drew & Lahey 1987; 1990]:

$$\mathbf{M}_c^L = C_L \epsilon_d \rho_c \nabla_r \times \nabla \times \nabla_c \quad (8)$$

The effects of the liquid turbulence interaction with particles/bubbles are included in the turbulent dispersion force:

$$\mathbf{M}_c^{(ND),TD} = -\mathbf{M}_d^{(ND),TD} = C_{TD} \rho_c k_c \nabla \alpha_d \quad (9)$$

### 2.2.2 Binary Collisions between the particles and the particle-wall collisions

Alajbegovic [1994] has developed closure laws for the stress induced in the dispersed phase and the transfer of the kinetic energy. For brevity only the procedure used to derive the expressions is described here. The following assumptions were made: collisions between more than two particles at the same instant are negligible; all collisions are elastic with negligible rotational effects. Starting from the expression for the average stress inside the dispersed phase given by Batchelor, [1970] an integral expression for the collision-induced shear stress is obtained by evaluating the probabilities of collisions of particles moving with given velocity, position and size. This expression is similar to that obtained by Chapman and Cowling [1970]. This was further integrated to obtain the final expressions. Similar procedure was used to calculate particle-wall collision-induced force.

### 2.2.3 Turbulent Interfacial Work

The interaction between the dispersed particles and the eddies is governed by the following equations:

$$\frac{dv'_i}{dt} p_{,i} = -\frac{1}{\tau_R} (v'_{p,i} - v'_{c,i}) \quad (10)$$

$$\frac{d}{dt} (m_c v'_c + m_p v'_p) = 0 \quad (11)$$

The interfacial work due to particle interactions with the continuous phase turbulence is:

$$W'_{d,ij} = \frac{\rho \alpha}{\tau_R} \left( C_1^W \overline{v'_{c,i} v'_{c,j}} - C_2^W \overline{v'_{p0,i} v'_{p0,j}} \right) \quad (12)$$

where,

$$\tau_R = \frac{4\rho_d D_p}{3\rho_c C_D |\nabla_p - \nabla_c|} \quad (13)$$

### 2.2.4 Algebraic Stress model for the dispersed phase Reynolds Stress

Starting with the assumption that:

$$\frac{v'_i v'_j}{k} \cong \text{const.} \quad (14)$$

and negligible collisions and small gradients in the dispersed phase's mean velocity, we obtain

$$\overline{v'_{d,i} v'_{d,j}} = C_{R,ij} \frac{k_d}{k_c} \overline{v'_{c,i} v'_{c,j}} \quad (15)$$

The above models have been tested against experimental data obtained at Rensselaer and elsewhere for various flow situations, and show remarkable accuracy.

## 3.0 Solid/Liquid Experiments

In a two-phase mixture for low volume fractions, the lift force is one of the most important phenomena affecting the radial distribution of the flow. This effect is due to the relative velocity between the two phases. Serizawa et. al. [1988] demonstrated that this lift force pushes bubbles towards the wall in upward flows and towards the center of the conduit for downward flows.

Figure-1 shows how the gravity affects the hydrodynamic behavior of a turbulent two-phase flow. We may eliminate the buoyancy force by using a dispersed phase of same density as that of continuous phase. Assad et. al. [1995] measured the liquid and dispersed phase distribution in a solid/liquid two-phase flow in a horizontal pipe using a Laser Doppler Anemometer (LDA). The dispersed phase consisted of ~2.0 mm average diameter size expanded polystyrene particles with specific gravity of 1.03. The test section was 30.6 mm in diameter and the pipe was made out of a special optically clear material (FEP, Fluorinated Ethylene Propylene) with the same index of refraction as water. Measurements for the velocity profile, turbulent structure and the volume fraction for each phase were made for various flow rates and global volume fractions.

The two-fluid model described above was incorporated into the PHOENICS code to test it against the data for neutrally buoyant particles. Although the model was developed for vertical flows, only, the neutral buoyant particle data for horizontal flows can still be compared against the calculations. Figure 3 shows that the agreement with data is good.

## 4.0 Liquid/Liquid Experiments

The particles which were used by Assad [1995] were solid spheres with a non-deformable, non-slip interface. The flow dynamics around them are well understood and documented. In case of bubbles and droplets, there is no solid interface; the fluid outside interacts with the fluid inside giving rise to internal circulations and deformations. Pressure differentials can deform the surface so that they are no longer spherical. All this affects the interfacial momentum transfer and the turbulence structure in a significant way. However, if the droplets/bubbles are small enough, the deformations are very small compared to their size and hence can be neglected. The liquid/liquid experiments allow us to further verify our models and

collect data to guide us in further enhancements.

Butyl benzoate was chosen as the dispersed phase for simulating microgravity. It has a specific gravity of 1.0 at 20° C. Also, it is more sensitive to temperature as compared to water. This makes it convenient to gravity separate the oil from water by heating the mixture by 20°C. It has since been shown to have satisfactory optical properties for Phase Doppler measurements.

The closed loop mode of operation was found to be unsuitable for obtaining mono-dispersed droplet flows. This motivated us to consider open loop operation with an injector to produce a mono-dispersed suspension. A droplet injector was designed and has been constructed with the following characteristics: (i) ability to control the flow rate of water, (ii) ability to control the diameter of the oil droplets, (iii) ability to control the relative flow rates of water and oil to obtain desired global void fraction, and (iv) most importantly, the droplet size distribution should be as small as possible. Indeed, we want a mono-dispersed flow so that a correlation between the size of the droplet and the phase distribution phenomenon may be established. The obvious choice to achieve the above objectives is to have capillary tubes as injection units. A preliminary calculation was done to predict the size of the droplets as a function of oil volume flow rate, velocity of the stream trying to shear off the droplets from the tips and the size of the capillary. This was guided by the work done by several researchers [Hayworth et. al., 1950; Null et. al., 1958] where a balance between the drag on the spherical droplet being formed at the tip due to the fluid motion and the cohesion forces due to surface tension yielded a correlation between the droplet size and the capillary size with fluid velocity as a parameter. This droplet injector has been tested and appears to be functioning as predicted.

During initial tests, LDA data was found to be inadequate to estimate the size of the droplets accurately. This inadequacy stems from the method of interpreting the transit time of a burst as an indicator of the size of the droplets. This mode of droplet size estimation can only be used to get an approximate idea of the size distribution. For more accurate data we may use a Fiber Phase Doppler Anemometer (FPDA) which relies on the phase difference between the reflected light detected by two detectors, a fixed distance apart, to determine the size of the droplet. A FEP conduit was used as the test section and both the probes were submerged under water so that the optical path length does not change when traverses are made.

## 5.0 The Experimental Facility

A batch mode oil/water loop was built and tested as shown in figure-2. To avoid the realignment of the FPDA probe at each measurement location, the probes and the FEP test section are all immersed in water so that no correction or alignment has to be done for measurements at different locations.

The oil droplet injector was tested to find out the effect of

oil and water flow rates on the size distribution of droplets. A small test loop was constructed outside of the main test facility for ease of observation and control. Following conclusions were drawn from the data obtained:

- (1). The droplet size decreases with an increase in water flow rate.
- (2). The average droplet size increases with the increase in oil flow rate and at the same time the spread in the size distribution increases.

## 6.0 Results and Discussion

A study was done to verify that an FPDA can measure oil droplet size. This was necessary to optimize the setup variables and verify the optical properties of oil in the context of the FPDA measurements. Figure-4 below shows the experimental facility used for this purpose. A small glass tank was filled with a known amount of water. It was determined that the reflection mode of diameter measurement is most suited for actual measurements. Two void fractions were measured: 0.07% and 0.21%. Larger void fractions could not be tried because of the formation of an emulsion by the stirrer. This increased the turbidity of the mixture to such a large extent that the measurement rate decreased by a factor of 10.

Figure-5(a) shows the seeding size distribution in which 3.5 cc of the seeding was used to seed 19.6 liters of water. A sample of the seeding was analyzed under a travelling microscope to determine the sizes present. The glass seeding sizes were found to be in the range 5  $\mu\text{m}$  to 100  $\mu\text{m}$ , with most of them in 25 to 50  $\mu\text{m}$  range. Although the data is not statistically representative of the distribution, it gave us the bounds on size. The histogram in figure-5(a) is accurate to that extent with most particles the same range as above. Optimization of the alignment and different parameters led to different trials with most of them resulting in the similar distribution.

Figure-5(b) shows the particle size distribution in unseeded water. The particles measured are the natural seeding suspended in the water supply. Most of the particles are in range 0 to 20  $\mu\text{m}$ . Figure-5(c) shows the oil droplet size distribution for a volume fraction of 0.07%. Immediately after the measurements were done with unseeded water, 15.5 cc of oil was added. The stirrer immediately broke up the oil globules into small droplets and a delay of about 10 minutes was allowed before measuring to allow the system to stabilize. The histogram in figure-5(c) shows the range of sizes present is 0 to 340  $\mu\text{m}$ . Most of the particles are below 100  $\mu\text{m}$  in diameter. If this is compared with the figure-5(b), it is practically impossible to say which of the data belong to the droplets and which to the natural seeding especially in the 0-25  $\mu\text{m}$  range. This is the case with low volume fraction, however at higher volume fraction, the data percentage in this range must be small to be able to neglect the influence of natural seeding. This was confirmed by adding more oil to the tank, the resulting void fraction being 0.2%. Figure-5(d) shows a typical data set obtained

at this volume fraction. Here most of the droplets are in range 40 to 100  $\mu\text{m}$  and the fraction of particles/droplets less than 20  $\mu\text{m}$  is very small. With the injector in the main loop, we should be able to keep the global void fraction relatively large enough without any emulsification. Thus we are confident that with large sample sizes, the data will be representative of the true droplet size distribution.

## 7.0 Proposed future work

The main thrust of the future work is to put an experiment aboard the space shuttle. The objective of the experiment is to measure phase separation in an air/water mixture. The emphasis is on simplicity and efficiency in conducting the experiment and to provide adequate instrumentation of acquire a complete set of data. These data can then be used for further understanding the dynamics of bubbly flows in space. The instrumentation will consist of: (i) a two-dimensional pen Laser Doppler probe; (ii) a Phase Doppler Anemometer; (iii) a real time Fast Fourier Transform system, a phase discriminator, a high voltage generator and a demodulator, all fitted on a single PC card; (iv) a one-dimensional hot film anemometer; (v) a traversing mechanism, and (vi) a CCD camera. We will measure two-dimensional velocities with the LDA, one dimensional velocities and the local void fraction with the hot film probe, size distribution of the bubbles with the CCD camera and the FPDA. All these will be measured as a function of radial position for two axial locations: one close to the inlet and one close to the outlet. These data will allow us to compute bubble coalescence and breakup as well as the developing phase distribution. These instruments will be progressively tested and calibrated in experiments in drop-towers and parabolic flights in Lear Jets. The loop itself will be a recirculating loop. A sine pump will circulate the mixture. For monodispersed experiments, we will separate the water from air using a centrifuge. For a arm length of 10 cm we will need about 600 rpm to simulate normal gravity. A specially designed injector will be used to generate the bubbles.

## 8.0 Bibliography

- Alajbegovic, A., "Phase Distribution and Turbulence Structure for Solid/Fluid Upflow in a Pipe", Ph.D. Thesis, Rensselaer Polytechnic Institute, Troy, New York, 1994.
- Arnold, G.S., "Entropy and Objectivity as Constraints Upon Constitutive Equations for Two-Fluid Modeling of Multiphase Flow", Ph.D. Thesis, Rensselaer Polytechnic Institute, Troy, New York, 1988.
- Assad, A., "An Experimental Study of Phase Distribution and Turbulence Structure for Solid/Liquid Flow in Horizontal and Vertical Pipes", Ph.D. Thesis, Rensselaer Polytechnic Institute, Troy, New York, 1995.
- Batchelor, G.K., "The Stress System in a Suspension of Force-Free Particles", *J. Fluid Mechanics*, Vol. 14, pp. 545-570, 1970.
- Chapman, S. Cowling, T.G., "The Mathematical Theory of Non-Uniform Gases", Cambridge University Press, Cambridge, 1970.
- Drew, D.A., Lahey, R.T., Jr., "The Virtual Mass and Lift Force on a Sphere in Rotating and Straining Inviscid Flow", *Int. J. Multiphase Flow*, vol. 13(1), pp. 113-121, 1987.
- Drew, D.A., Lahey, R.T., Jr., "Some Supplemental Analysis on the Virtual Mass and Lift Force on a Sphere in Rotating and Straining Inviscid Flow", *Int. J. Multiphase Flow*, vol. 16(6), pp. 1127-1130, 1990.
- Drew, D.A., Passman, S.L., "Theory of Multicomponent Fluids", To be published, 1995.
- Hayworth, Curtis B, and Treybal, Robert E., "Drop Formation in Two-Liquid-Phase Systems", *Industrial and Engineering Chemistry*, Vol. 42, No. 6, June 1950.
- Lahey, R.T., Jr., Drew, D.A., "The Current State-of-the-Art in the modelling of Vapor/Liquid Two-Phase Flows", *ASME 90-WA/HT-13*, 1990.
- Nigmatulin, R.L., "Spatial Averaging in the Mechanics of Heterogenous and Dispersed Systems", *Int. J. Multiphase Flow*, vol. 5, pp. 353-385, 1979.
- Null, Harold R., and Johnson, Homer F., "Drop Formation in Liquid/Liquid Systems from Single Nozzles", *A.I.Ch.E. Journal*, Vol. 4, No. 3, Sept. 1958.
- Park, J-W., "Void Wave Propagation in Two-Phase Flow", Ph.D. Thesis, Rensselaer Polytechnic Institute, Troy, New York, 1992.
- Serizawa A., Kataoka I., "Phase Distribution in Two-Phase Flow", *Transient Phenomena in Multiphase Flow*, Ed. Afghan, N.H., Hemisphere Pub. Corp., New York, pp. 179-225, 1988.

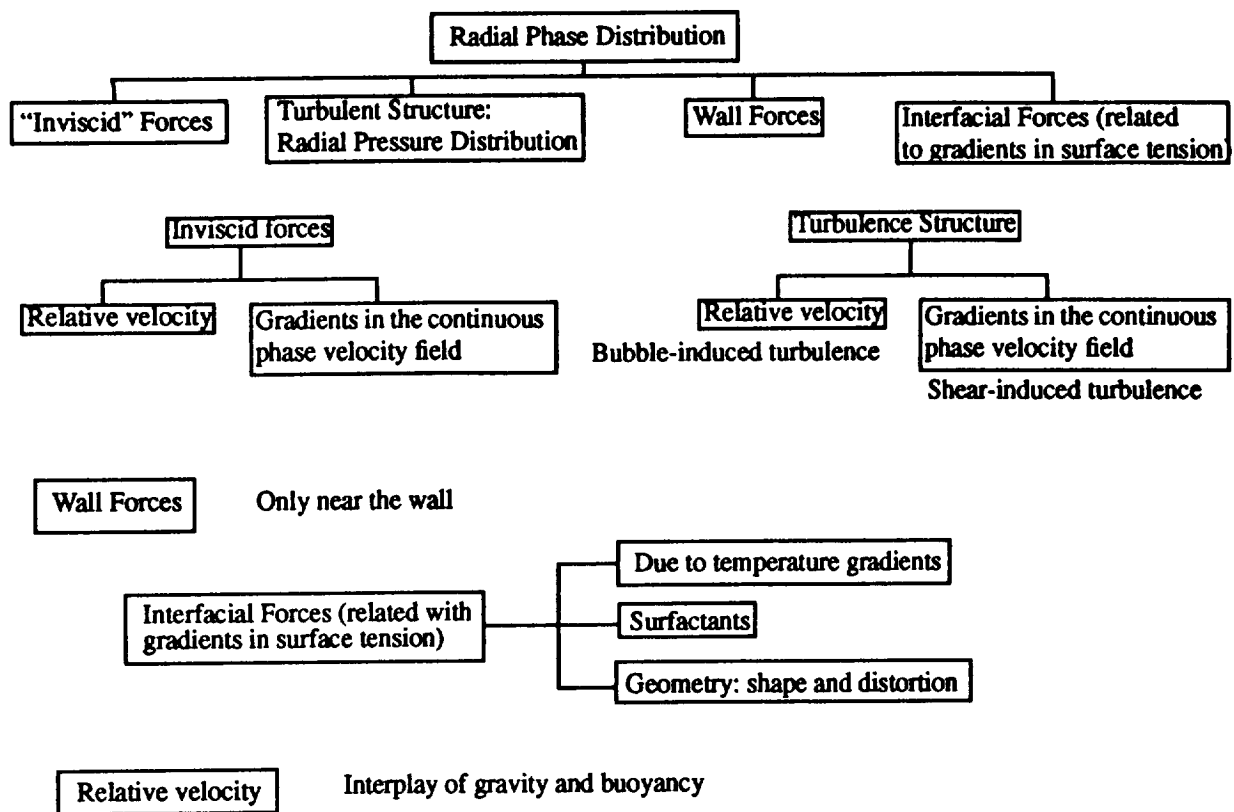


Fig. 1. Parametric dependence of two fluid models

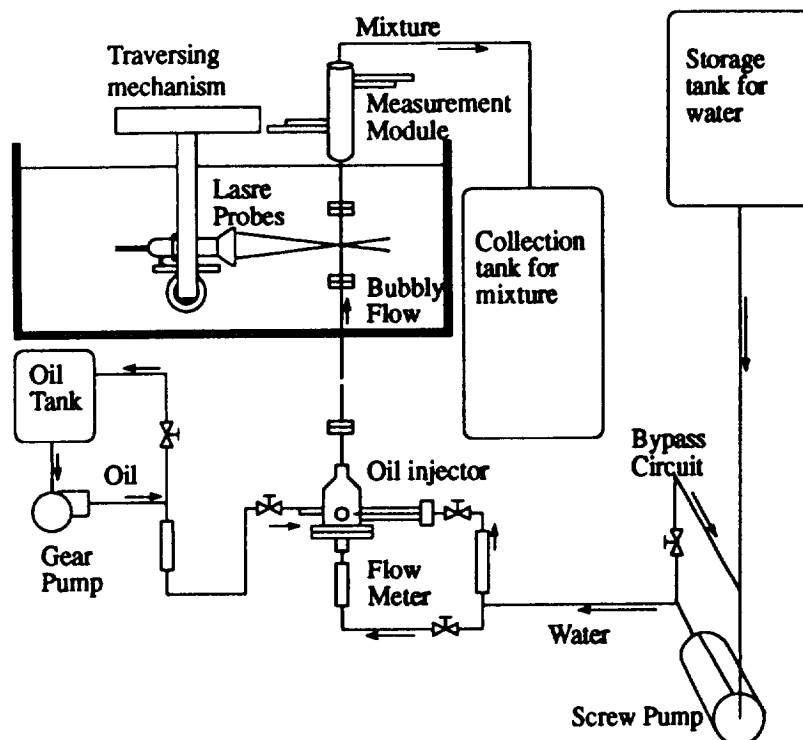


Fig. 2. Schematic of the new facility.

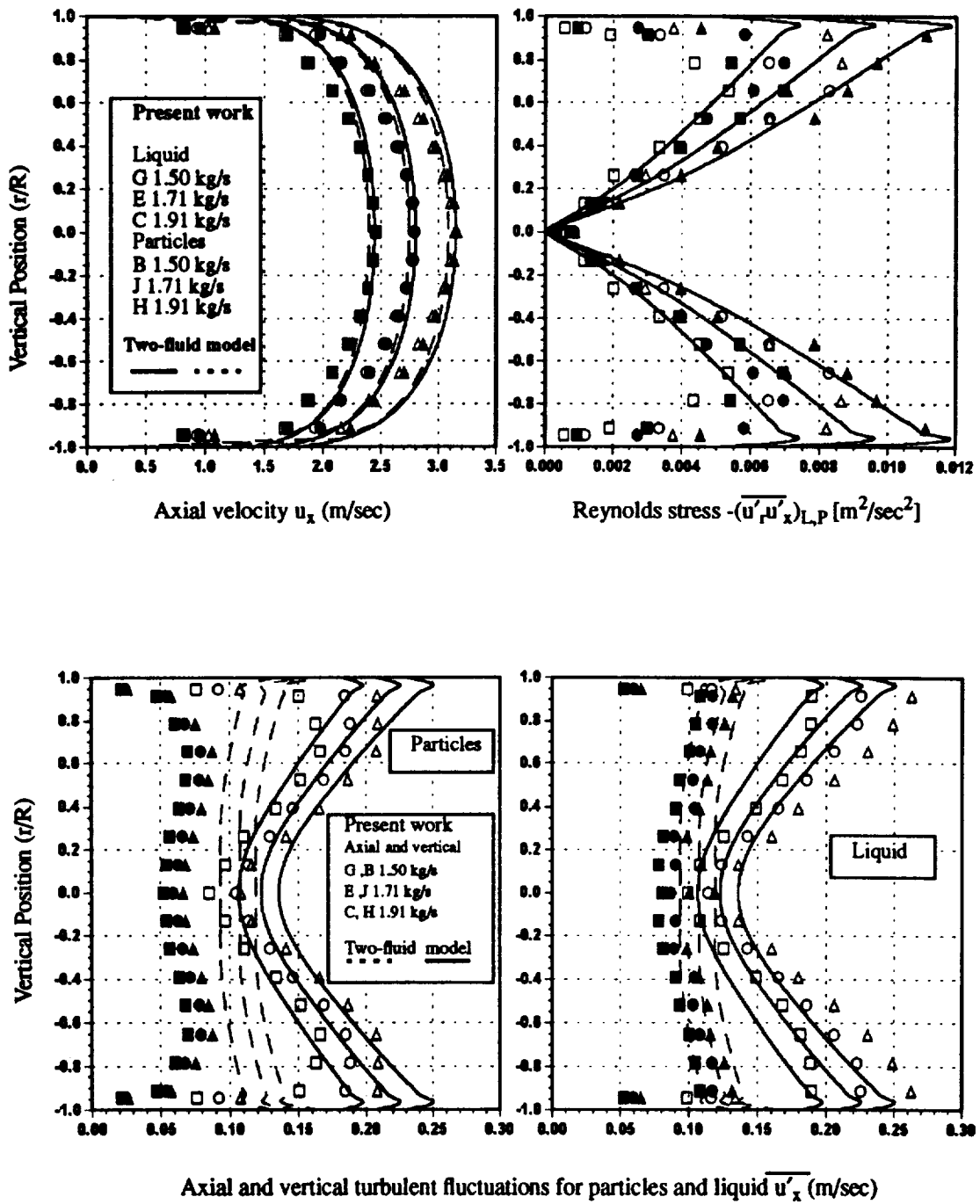


Fig. 3. Comparison between measured and predicted velocity and turbulence quantities for neutral particles.

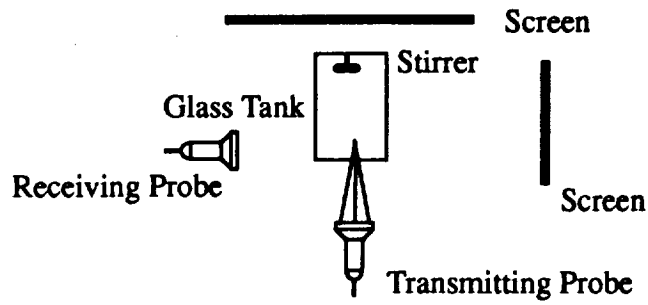
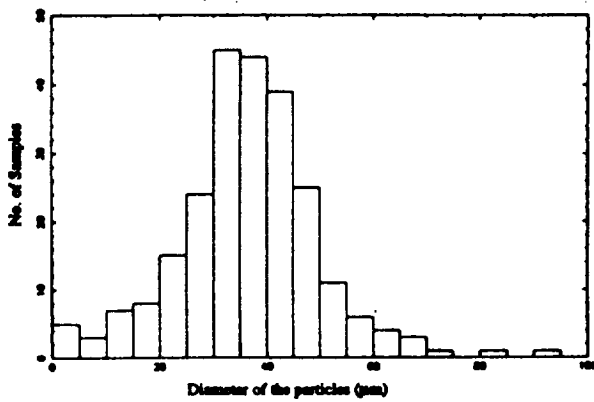
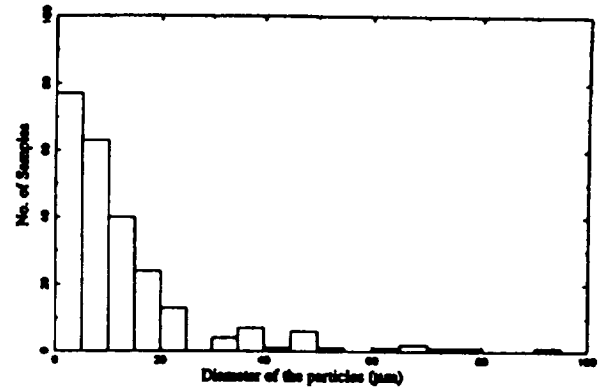


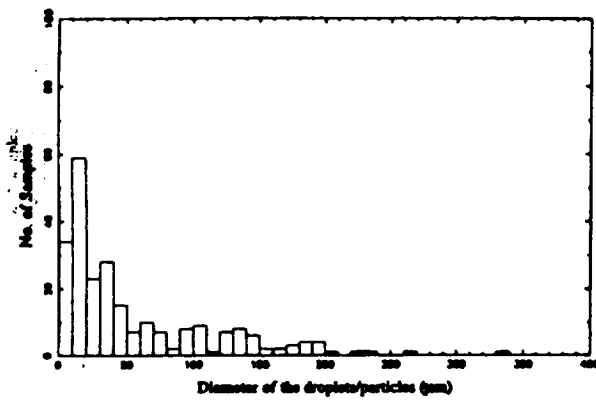
Fig 4. Schematic of the FPDA trial setup.



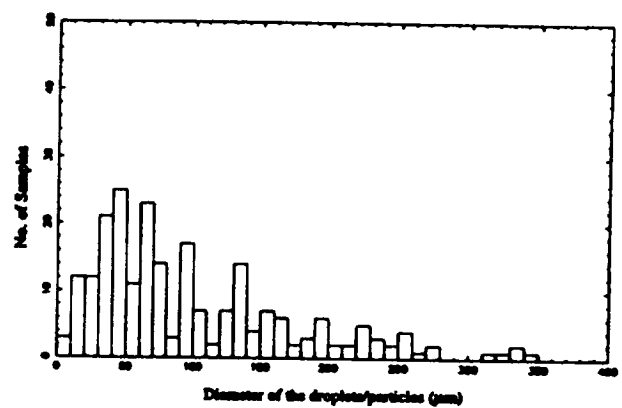
(a) With glass seeding



(b) Unseeded Water



(c) Oil droplets, Global void fraction=0.08%



(d) Oil droplets, Global void fraction=0.21%

Fig. 5. Particle/droplet size distributions.

